

Oct 20th, 12:00 AM

Unstiffened Elements - Some Interesting Features

J. Rhodes

Follow this and additional works at: <https://scholarsmine.mst.edu/isccss>



Part of the [Structural Engineering Commons](#)

Recommended Citation

Rhodes, J., "Unstiffened Elements - Some Interesting Features" (1992). *International Specialty Conference on Cold-Formed Steel Structures*. 2.

<https://scholarsmine.mst.edu/isccss/11iccfss/11iccfss-session1/2>

This Article - Conference proceedings is brought to you for free and open access by Scholars' Mine. It has been accepted for inclusion in International Specialty Conference on Cold-Formed Steel Structures by an authorized administrator of Scholars' Mine. This work is protected by U. S. Copyright Law. Unauthorized use including reproduction for redistribution requires the permission of the copyright holder. For more information, please contact scholarsmine@mst.edu.

Unstiffened Elements- Some Interesting Features

Jim Rhodes*

Summary

The behaviour of members composed of unstiffened elements is examined with reference to three different sets of test results, on angle section struts, Tee section beams and shallow Vee section beams. The test results are explained on the basis of fairly simple analysis, and the variations of the behaviour from that predicted by modern design codes is discussed.

Introduction

The behaviour of unstiffened elements, and the effects of this behaviour on the strength and stiffness of members, has been a source of doubt and some controversy for many years. The fundamental differences in the behaviour unstiffened elements in comparison with stiffened elements arise in the facts that:-

- (a) The buckling stress for unstiffened elements is substantially lower than for stiffened elements.
- (b) The variation in buckling stress with variation in edge restraint on rotation is significantly larger in unstiffened elements than in stiffened elements.
- (c) While a stiffened element loses effectiveness largely from its central portion after buckling in compression an unstiffened element loses effectiveness of the unstiffened edge, and the resistance to further load becomes eccentric, thus inducing bending under many circumstances. The effective neutral axis of an unstiffened element moves substantially towards the supported edge while for a uniformly compressed stiffened element the effective neutral axis remains relatively constant.

The relatively low local buckling resistance of unstiffened elements and the subsequent localisation of compression resistance at the supported edge has very significant effects on the behaviour of beams and columns which are composed largely of such elements. It is always desirable to minimise the use of slender unstiffened elements if at all possible.

On the other hand, from the viewpoint of understanding the mechanics of the behaviour of thin-walled sections, the fact that unstiffened elements display these undesirable traits allows the researcher to obtain a good insight into buckling behaviour and similar effects. In this paper, tests on members composed completely of unstiffened elements are examined, and some of the results are shown to be rather surprising, but of interest and importance in the study of cold formed members. Three particular cases are examined, angle sections under eccentric compression, shallow Vee beams under pure bending and Tee sections in bending.

Professor, Department of Mechanical Engineering, University of Strathclyde, Glasgow, Scotland.

Angles subjected to eccentric compression

Angle section struts are most interesting members inasmuch as the local buckling mode for these members is identical to the torsional buckling mode. When such members buckle in torsional-flexural buckling then, if the slenderness ratio is not great, torsion is the dominant feature of the torsional-flexural buckling mode, and thus the local buckling stress is very close to the torsional-flexural buckling load.

In the AISI Specification (1) and the British standard (2) the capacity of such members can be evaluated on the basis of torsional-flexural buckling analysis. Since the torsional buckling could also be termed local buckling in this case, however, it would also seem logical that the struts could be analysed as columns under combined bending and compression, with the effective area evaluated on the basis of the local (or torsional) buckling of the elements. This would be permissible in design to the British Code, although the AISI specification specific rules are given for angles which preclude such design. It is of interest in any case to ascertain which approach is more accurate in comparison with tests.

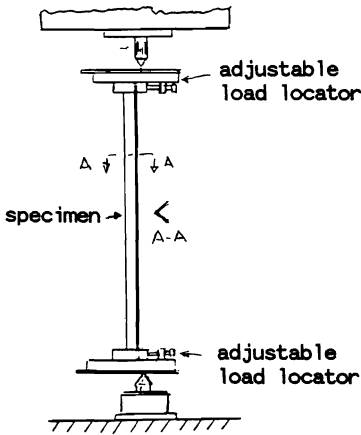


Figure 1. Test setup

To this end, a series of 26 tests was carried out recently (3) on equal angle section struts loaded in combined compression and bending, with load applied on the axis of symmetry at various eccentricities to the neutral axis. The angles were all of the same nominal dimensions, 25 mm leg width, 0.8 mm thickness and 382 mm length. All specimens were manufactured from the same sheet of material and the measured yield strength was 295 N/mm². End loading fixtures were manufactured to allow free movement of the ends in all directions, but to apply the loading at a specified eccentricity to the neutral axis. The test layout is shown diagrammatically in Figure 1. Loads were applied at eccentricities ranging from +30mm to -30mm at 5mm intervals. For each load eccentricity two specimens were tested. The failure loads for all tests are given in Table 1.

Torsional-flexural buckling analysis is treated comprehensively in refs (4) and (5). For a section with pinned ends subject to an eccentric load the Torsional-flexural buckling load is:

$$P_{TF} = \frac{1}{2\beta} \left\{ (P_{ex} + P_T) \pm \sqrt{(P_{ex} + P_T)^2 - 4\beta P_{ex} P_T} \right\} \quad (1)$$

For positive loading eccentricities (ie loading towards the free edges of the section) the lower root of this equation governs. For negative loading eccentricities the failure load corresponding to combined flexural buckling and yield has a lower value than given by equation (1), so that this mode governs for such eccentricities. This mode of failure occurs at a load P given by the interaction equation

$$\frac{P}{P_S} + \frac{P e_x}{M_c(1 - P/P_{ey})} = 1 \quad (2)$$

Equation (2) can be solved swiftly by iteration.

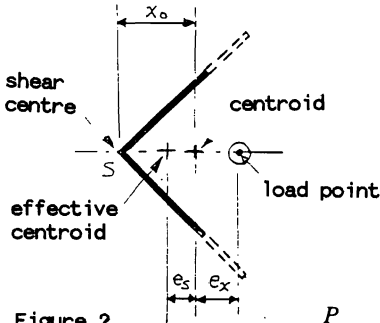
If the problem is examined on the basis of local buckling, using the British design code, then

the short strut squash load is found from

$$P_{cs} = \sigma_Y A_{eff} \tag{3}$$

The effective area is obtained by evaluating the effective widths of the legs, and summing the effective areas of both legs. In the British Standard the interaction of local and overall buckling is taken care of by the application of the Perry-Robertson equation

$$P_c = \frac{1}{2} \left\{ (P_{cs} + (1 + \eta)P_{ey}) - \sqrt{(P_{cs} + (1 + \eta)P_{ey})^2 - 4P_{cs}P_{ey}} \right\} \tag{4}$$



Since the effective neutral axis position is not the same as the neutral axis position for the gross cross section, as illustrated in Figure 2, then the change in effective eccentricity caused by this movement of the neutral axis should be incorporated into the analysis. This is the well known "wandering neutral axis" concept. For the interaction of axial load and bending the relevant equation is

Figure 2

$$\frac{P}{P_c} + \frac{P(e_x + e_s)}{M_{cR}(1 - P/P_{ey})} = 1 \tag{5}$$

This equation is similar to equation (3), with the alterations that the effective area and effective moment resistance replaces the gross area and gross moment resistance, while the moment considered takes into account the movement of the neutral axis.

Figure 3 shows a comparison of the results of both torsional-flexural analysis and effective width analysis with the experimental failure loads for the range of loading eccentricities.

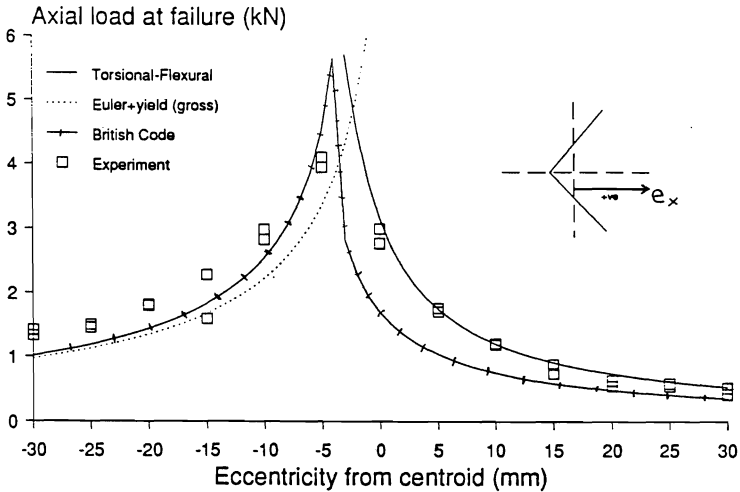


Figure 3. Eccentrically compressed angle

There are several interesting observations which can be made on the basis of this figure. For negative eccentricities the torsional-flexural buckling load accurately describes the failure loads, with a small degree of non-conservatism, while the failure load based on the effective width approach is conservative, but less accurate. It is worthy of note that the local buckling load for the sections considered, based on plate analysis, is almost identical with the torsional-flexural buckling load. The local buckling stress calculated on the basis of plate theory is

$$\sigma_{cr} = K \frac{\pi^2 E}{12(1-\nu^2)} \left(\frac{t}{b} \right)^2 \quad (6)$$

$$\text{where } K = \frac{1.7}{3+R} \quad \text{with } R = \frac{2.946 + e_x}{2.946 - e_x}$$

In the particular case of a uniformly compressed section, taking Poisson's ratio as 0.3, plate analysis gives the critical stress as $2.603 E (t/b)^2$ while beam theory gives the torsional-flexural buckling stress as $2.6 E (t/b)^2$, ie almost identical. Thus for this case beam theory and plate theory are almost co-incident.

In the case of negative eccentricities an important point emerges. Here, for the smallest negative eccentricity the analysis based on the gross area underestimates experiment slightly, while analysis based on effective area and wandering neutral axis actually overestimates the capacity. Thus in this instance taking account of the change in neutral axis position can lead to unsafe design. In considering the behaviour of a strut with a negative eccentricity, it is noticeable that the eccentric loading decreases the stress at the free edges, and thus delays, and perhaps eliminates, local buckling. In such a case the neutral axis position does not change although analysis of the strut as a uniformly compressed member suggests that local buckling, and neutral axis movement, would occur. Therefore taking neutral axis movement into account does not necessarily ensure safer analysis in all cases. Other instances in which the wandering neutral axis must be examined carefully have emerged in recent times (6), (7), and as an early proponent of this effect the author must issue the warning to treat this effect with care. As a first step, it would be advisable for design codes to specify that analysis should consider the load capacities obtained if neutral axis movement is taken into account and if it is not taken into account, and take the lower of the values obtained.

Shallow Vee section beams

Some design specifications have inbuilt limitations on the geometries for which the standard analysis techniques can be applied. The British code, for example, does not apply to members which have elements with bend angles greater than 135 degrees. This is due to the fact that with these large bend angles the behaviour is influenced by a number of factors.

To examine one of these factors a series of tests was carried out a few years ago on shallow Vee cross section beams (8). Thirty six beams were tested to failure under pure bending, with 18 beams bent in such a way that the free edges were in tension and the other 18 bent to cause tension of the free edges, as illustrated in Figure 4.

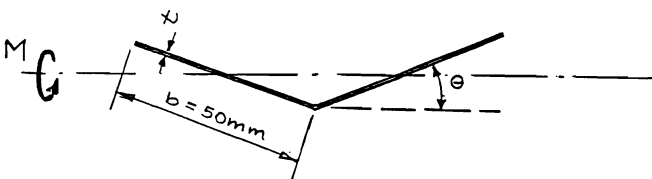


Figure 4. Shallow vee beam

The flange angles of the beams tested, measured from the horizontal, varied from 5 degrees to 28 degrees, so that the bend angles varied from 124 degrees, within the British code, to 170 degrees. All specimens had nominal flange widths of 50mm. The dimensions and geometry, yield stresses and ultimate moments for all specimens are given in Table 2. In this table members designated VT were bent to cause tension of the free edges, and members designated VC were bent to cause compression of the free edges.

In the case of the members bent to cause tension of the free edges the sections were fully effective with regard to bending, and the ultimate moment based on design analysis is equal to the moment to cause first yield. Figure 5 shows comparisons of the predicted failure moments with the failure moments obtained from test. The predicted moments overestimate the actual capacity for very shallow members, and underestimate the capacity for deeper members. The degree of overestimation for shallow members is substantial, with the predictions being more than 100% greater than the actual failure moments. For the deeper cross sections the predictions underestimate the capacity by up to 30%. The reasons for these discrepancies lies in two factors, (1) the neglect of elasto plastic post yield capacity in the deeper sections and (2) the neglect of section flattening effects in the shallow cross sections.

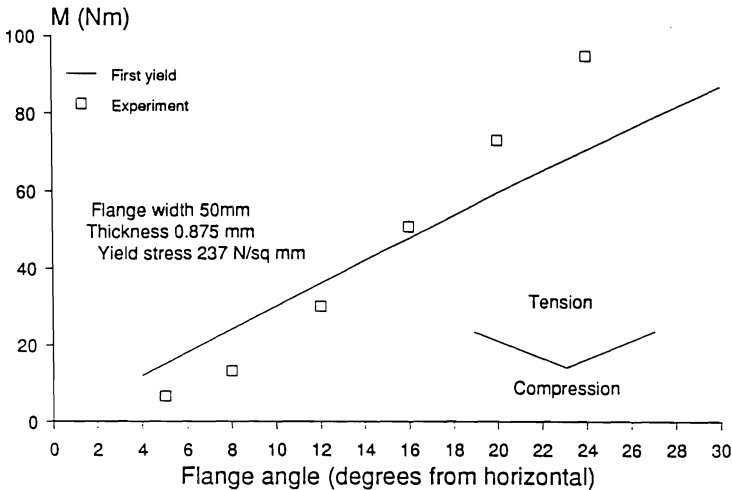


Figure 5. Moment capacity for Vee beams

Flattening of the member cross section can be taken into account by assuming a deflected form across the section as shown in Figure 6.



Figure 6. Cross-section deflections

Assuming that the deflected form is given by the expression

$$w = A \left(\frac{s}{b} \right)^2 \quad (7)$$

the second moment of area of the deformed cross section, and the neutral axis location can be evaluated as

$$\bar{y} = \frac{b}{2} \sin \theta - \frac{A}{3} \cos \theta \quad (8)$$

$$I_{NA} = 2bt \left[\frac{b^2}{12} \sin^2 \theta + \frac{4}{45} A^2 \cos^2 \theta - \frac{1}{12} Ab \sin 2\theta \right] \quad (9)$$

The energy of the cross section bending can be obtained simply and approximately as

$$V_b = \frac{2}{3} E I A^2 \left(\frac{t}{b} \right)^3 \quad (10)$$

The total strain energy in a beam bent to a curvature C is then

$$V = E I C^2 l - \frac{2}{3} E I A^2 \left(\frac{t}{b} \right)^3 \quad (11)$$

from the principal of minimum potential energy, in the present case the strain energy must be a minimum if the curvature is specified. Thus substituting for I from equation (9), differentiating equation (11) with respect to C and setting the result equal to zero yields

$$A = \frac{\frac{15}{32} b \sin 2\theta}{\cos^2 \theta + 15t^2/4C^2b^4} \quad (12)$$

The moment M can now be related to the curvature by the equation

$$M = EIC = 2Ebt \left[\frac{b^2}{12} \sin^2 \theta - \frac{4}{45} A^2 \cos^2 \theta - \frac{1}{12} Ab \sin 2\theta \right] \quad (13)$$

now for any curvature, C , the cross-beam deflection can be obtained from equation 12, the applied moment from equation 13 and the maximum stress can be evaluated with the help of equations 8 and 9. Thus the elastic behaviour can be examined. If it is assumed that after yield the elasto-plastic behaviour can be determined on the basis of elasto-plastic analysis of the current cross section corresponding to a given curvature, then the moment for a given strain at the extreme fibres can be obtained in terms of the elastically calculated moment from

$$m_{ep} = m \left[1 - 0.5 \left(1 - \frac{\epsilon_y}{\epsilon} \right)^2 \left(2 + \frac{\epsilon_y}{\epsilon} \right) \right] \quad (14)$$

The moment-curvature variation predicted from this analysis for a typical beam is shown in Figure 7. The elastically evaluated moment deviates from linear analysis as the curvature increases, and when yield is exceeded the elasto-plastic moment deviates from the elastic moment. Failure occurs when the elasto-plastic moment reaches its maximum value.

For very shallow beams the elastic moment and elasto-plastic moment are the same, ie the beam fails elastically due to cross section flattening. For deeper beams there are effects of flattening present before yield, which cause the moment-curvature variation to be non-linear to some extent before the onset of yield. For very deep beams the flattening effect becomes small, and yielding is the major cause of failure.

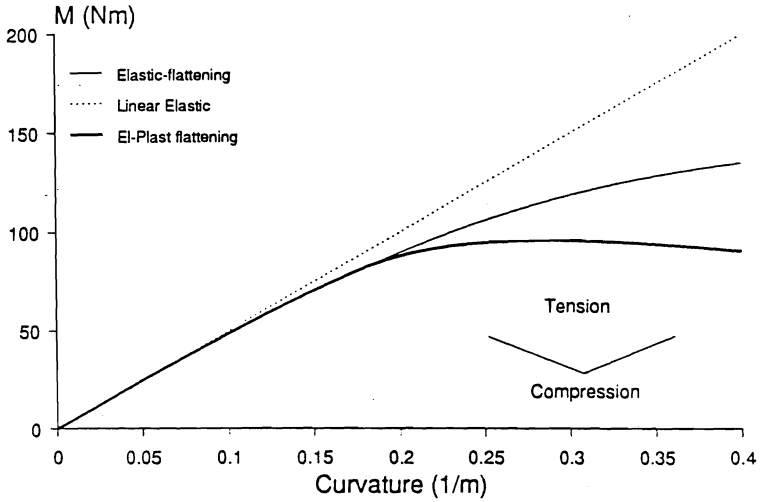


Figure 7. Moment-curvature for Vee beams

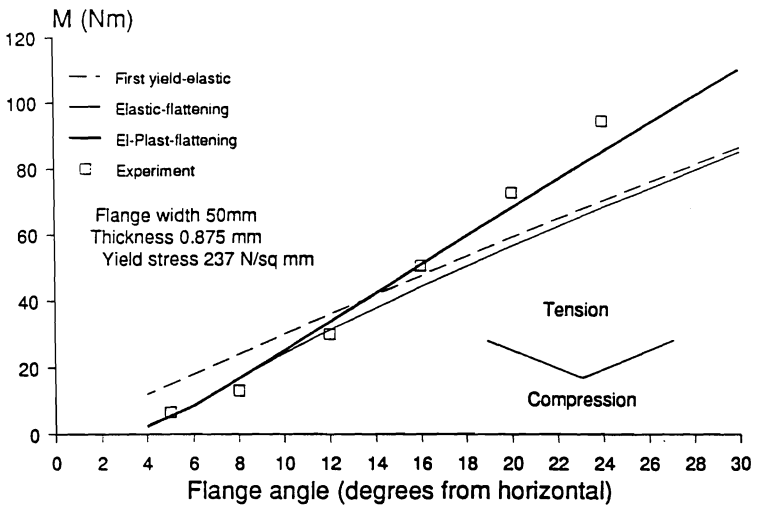
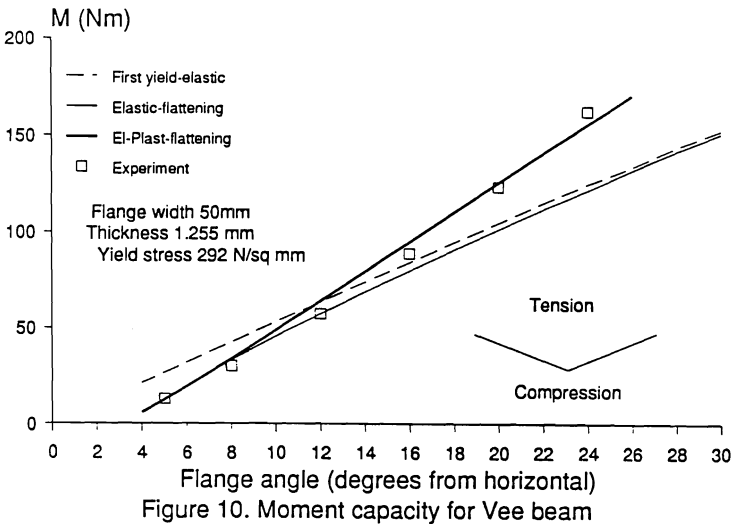
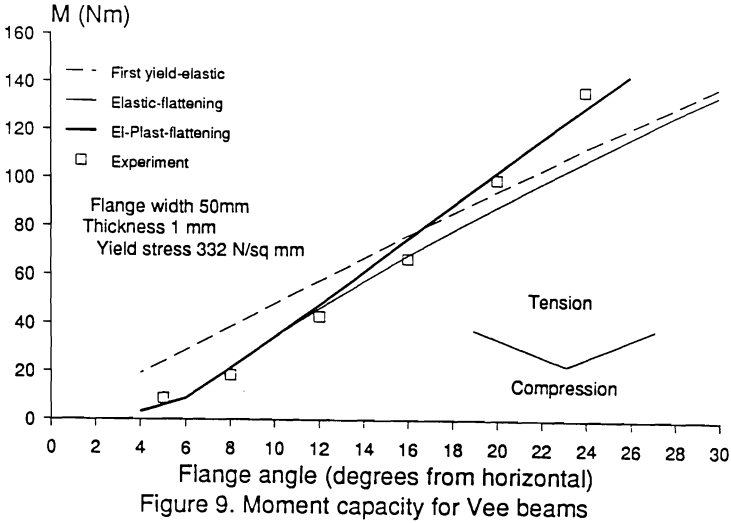


Figure 8. Moment capacity for Vee beams

Figure 8 shows the failure moments evaluated on this basis compared to the experimental results previously shown in Figure 6. The reduction in capacity for shallow beams due to flattening and the increase in capacity for deeper beams due to post yield capacity is modelled very well by the analysis. Figures 9 and 10 show comparisons for the other beams tested in this way, with again very good agreement with the experimental failure loads in both cases.



Interesting features of this investigation are that the cross section flattening effects can be extremely severe for members with large angles between the flanges, and that, although the elements were slender, for relatively deep cross sections the moment capacity approaches the fully plastic capacity.

Tee section beams.

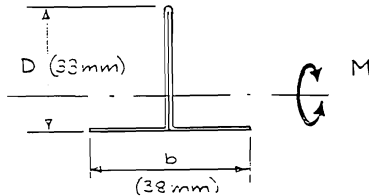


Figure 11. Tee section

The behaviour of tee section beams, as illustrated in Figure 11 was examined in a series of tests (9) some time ago. The lateral-torsional buckling of this type of beam is given by the following equation (2)

$$M_E = \frac{\pi^2 A E D}{2(L_E/r_y)^2} C_b C_T \left[\sqrt{1 + \frac{1}{20} (L_E t / C_T r_y D)^2} \pm 1 \right] \quad (15)$$

The sign after the square root is + if bending causes tension at the free edge of the vertical leg and - if bending causes compression here. In the British code the interaction of yield and lateral torsional buckling is taken into account using the Perry-Robertson formulation as given in Equation 4, with the overall buckling load and short strut squash load replaced by the Lateral-Torsional buckling moment and first yield moment respectively. The resulting moment capacity is termed M_b .

Figure 12 shows a comparison of the theory with test results for the case of bending which applies compression to the free edge of the vertical leg. In the analysis the effective length of the beams was taken as 0.9 times the span length, to take account of the restraint on lateral movement which resulted from the load application method.

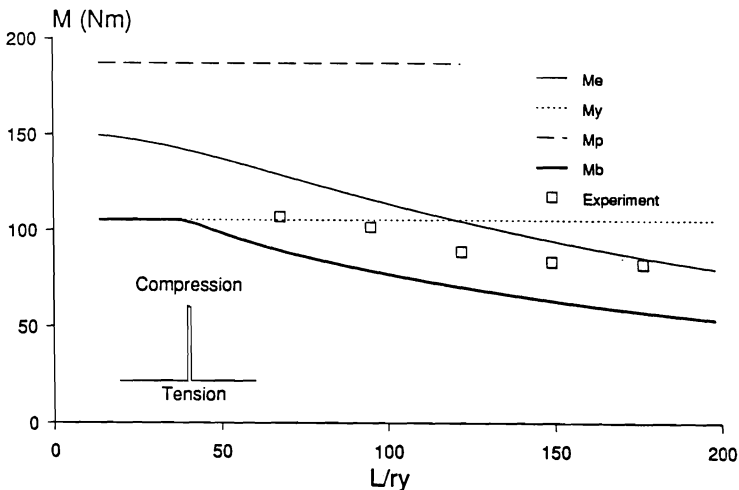


Figure 12. Ultimate moments for Tee beam

The analysis gives conservative estimates for the ultimate moment. Of perhaps greater interest in this case is the fact that for all of the beams tested failure resulted from *buckling of a tension element*. This strange effect arose from the initial torsional flexural buckling of the beam, which proved to be stable, and the beam resisted further load while its cross section deflected laterally and twisted substantially as shown in Figure 13. The horizontal legs, which were initially in tension, became subject to combined bending and axial force until the leg which had greatest compression buckled plastically, causing failure of the beam.

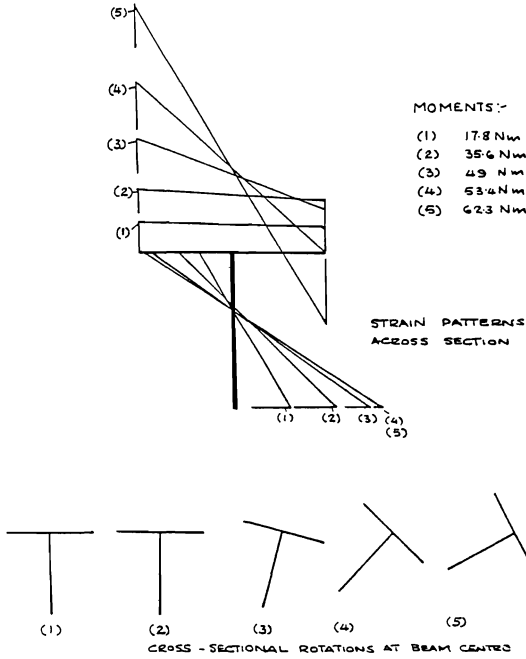


Figure 13. Strain distributions and rotations of tee beam

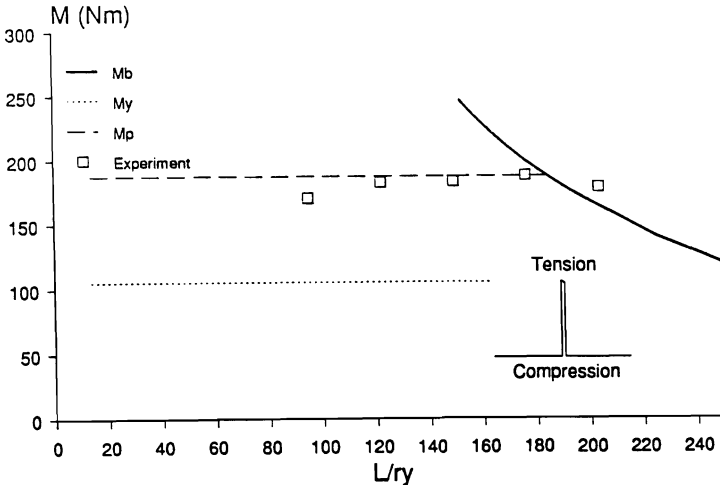


Figure 14. Ultimate moments for Tee beam

The theoretical results for beams bent in the opposite direction, ie to cause compression of the horizontal legs, are compared with experiment in Figure 14. Here lateral torsional buckling was not substantially evident and only the longest span was affected by this phenomenon. More interesting in this case is the fact that all specimens took moments substantially greater than the first yield moment. Indeed for all specimens the failure moment was close to the fully plastic moment, which for these sections is about 70% greater than the first yield moment. In this case the stresses on the compression elements were very much less than the maximum tensile stress in the elastic range, and these elements had a substantial degree of rotational restraint, although their b/t ratio was well over the lower limit for which local buckling would have to be considered.

Summary

The tests and analysis outlined here have shown a number of interesting effects. From the study of angles subjected to combined bending and axial load it has been shown that beam analysis and plate analysis for such sections leads to similar results. Taking account of neutral axis movement was shown to require careful treatment if a section is loaded in such a way that the neutral axis movement is in the direction which reduces the effective load eccentricity. In such cases it is possible that treatment of the column as being fully effective, with eccentricity measured from the original neutral axis will result in lower calculated load capacity than if the effective cross section and neutral axis position are used.

The examination of shallow vee section beams has illustrated that for sections with large angles between adjacent elements bending can cause flattening to a significant degree, with reduction in the moment capacity of these sections. This examination also showed that even slender members can have a significant post yield capacity. It should be mentioned here that in this case yield occurred both in tension and in compression.

The tests on tee section beams with moment to cause tension on the free edge of the vertical leg suggested that thin sections can sustain tensile strains far greater than the yield strain. The tests on tees with moment acting in the opposite directions indicate that, with large deformations, the loading on individual elements can change character, so that an element initially subject to tension can fail by compressive buckling.

Appendix 1. References

1. Specification for the design of cold formed steel structural members, August 1986 Edition. American Iron and Steel Institute, Washington DC.
2. BS 5950:Part 5. Code of practice for the design of cold formed sections. British Standards Institute, 1987.
3. Ong Wee Meng. "Behaviour of angle sections in combined compression and bending". B. Eng. Thesis, University of Strathclyde, May 1992.
4. Pekoz, T and Celebi, N. "Torsional-flexural buckling of thin-walled sections under eccentric load". Cornell University Engineering Research Bulletin 69-1, 1969.
5. Yu, W. W. "Cold Formed Steel Design". John Wiley and Sons, 1991.

- 6 Lim, K. W. "Examination of the effects of local buckling on the behaviour of fully fixed thin-walled columns". M Phil Thesis, University of Strathclyde 1987.
- 7 Loughlan, J. "Thin-walled cold formed sections subject to compressive loading." To be published in ThinWalled Structures, Special Issue on Cold Formed Steel Design, Eds W W Yu and J Rhodes
- 8 Rhodes, J. "Research into the mechanical behaviour of cold-formed sections and drafting of design rules". Report to ECSC, June 1987.
- 9 Rhodes, J. "Unstiffened Elements". Report to the Cold Rolled Sections Association, February 1985.

Appendix 2. Notation

A	Plate deflection magnitude
A_{eff}	Effective cross sectional area of a section
b	Width of a tee beam, or width of an element of a vee section
C_b	Moment variation factor
C_T	Coefficient for a tee section, equal to
D	Depth of a tee section
E	Modulus of Elasticity
e_x	Eccentricity of axial load from the centroid
e_s	Neutral axis movement in an effective cross section
I, I_{NA}	Second moment of area about the neutral axis
l	Length of a vee beam
L_E	Effective length of a tee beam
M	Moment
M_c	Moment capacity
M_{cR}	Moment capacity for a reduced effective cross section
M_E	Elastic lateral buckling moment
M_{ep}	Elasto-plastic moment
M_p	Fully plastic moment
P	Axial load
P_c	Column buckling load
P_{cs}	Short strut failure load, in the presence of local buckling
P_{ex}, P_{ey}	Euler buckling loads for buckling about the x and y axes
P_T	Torsional buckling load
P_{TF}	Torsional-flexural buckling load
P_S	Squash load
V_b	Bending energy
V	Total potential energy
w	Plate deflection
\bar{y}	Neutral axis position
ϵ	Strain
ϵ_y	Yield strain
η	Imperfection parameter in Perry-Robertson equation
σ	Stress
σ_{cr}	Critical stress to cause local buckling
ν	Poisson's ratio

Table 1. Failure loads for eccentrically loaded angles

SPECIMENS	TEST 1 FAILURE LOAD (N)	TEST 2 FAILURE LOAD (N)	AVERAGE TEST RESULTS
SC	2766.00	2992.92	2879.48
SR1 $e_x=5$	1755.56	1701.12	1728.34
SR2 10	1201.31	1185.84	1193.58
SR3 15	742.44	876.49	809.47
SR4 20	629.01	543.94	586.48
SR5 25	582.61	541.36	561.99
SR6 30	518.16	417.62	467.89
SL1 $e_x=-5$	3946.79	4104.04	4025.42
SL2 -10	2822.82	2982.65	2902.74
SL3 -15	2278.88	1590.57	1934.73
SL4 -20	1814.85	1794.23	1804.73
SL5 -25	1497.77	1451.37	1474.57
SL6 -30	1327.60	1412.70	1370.15

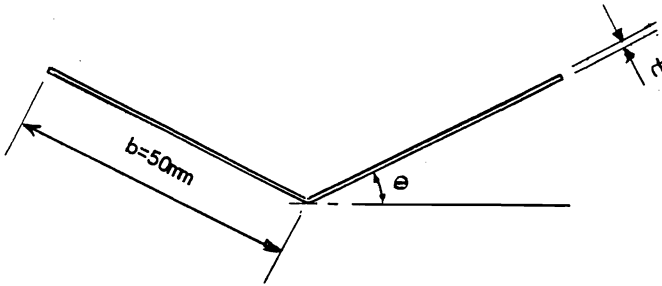
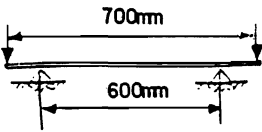


Table 2. Failure loads for vee beams

Spec No.	t mm	θ degrees	σ_Y N/mm ²	M_{ult} Nm
VT1	0.875	5	237	6.67
VT2	0.884	8	237	13.23
VT3	0.881	12	237	30.03
VT4	0.883	16	237	50.71
VT5	0.877	20	237	72.95
VT6	0.875	24	237	94.75
VT7	1.003	5	332	8.90
VT8	1.001	8	332	18.46
VT9	1.002	12	332	42.93
VT10	0.999	16	332	66.72
VT11	1.005	20	332	99.64
VT12	1.003	24	332	137.0
VT13	1.257	5	292.5	12.90

Table 2 - Continued

Spec No.	t mm	θ degrees	σ_Y N/mm ²	M_{ult} Nm
VT14	1.256	8	292.5	30.03
VT15	1.253	12	292.5	57.38
VT16	1.254	16	292.5	88.96
VT17	1.258	20	292.5	123.44
VT18	1.257	24	292.5	162.36
VC1	0.873	8	237	7.45
VC2	0.859	12	237	14.46
VC3	0.882	16	237	20.24
VC4	0.869	20	237	22.24
VC5	0.871	24	237	32.47
VC6	0.860	28	237	35.59
VC7	1.002	8	332	10.34
VC8	1.001	12	332	18.90
VC9	1.001	16	332	28.69
VC10	1.002	20	332	35.36
VC11	1.002	24	332	44.48
VC12	1.00	28	332	52.27
VC13	1.249	8	292.5	19.35
VC14	1.253	12	292.5	29.58
VC15	1.255	16	292.5	40.03
VC16	1.255	20	292.5	52.27
VC17	1.258	24	292.5	65.61
VC18	1.252	28	292.5	74.84

